Optics Letters

Heteroclinic dynamics of coupled semiconductor lasers with optoelectronic feedback

S. Shahin,[1,*,†] F. Vallini,[1,†] F. Monifi,[1,†] M. Rabinovich,[2] and Y. Fainman[1]

[1]Department of Electrical and Computer Engineering, University of California, San Diego, 9500 Gilman Drive, La Jolla, California 92093-0407, USA
[2]Institute for Nonlinear Science, University of California, San Diego, 9500 Gilman Drive, La Jolla, California 92093-0407, USA
*Corresponding author: shshahin@ucsd.edu

Generalized Lotka–Volterra (GLV) equations are important equations used in various areas of science to describe competitive dynamics among a population of N interacting nodes in a network topology. In this Letter, we introduce a photonic network consisting of three optoelectronically cross-coupled semiconductor lasers to realize a GLV model. In such a network, the interaction of intensity and carrier inversion rates, as well as phases of laser oscillator nodes, result in various dynamics. We study the influence of asymmetric coupling strength and frequency detuning between semiconductor lasers and show that inhibitory asymmetric coupling is required to achieve consecutive amplitude oscillations of the laser nodes. These studies were motivated primarily by the dynamical models used to model brain cognitive activities and their correspondence with dynamics obtained among coupled laser oscillators. © 2016 Optical Society of America

Competition and cooperation occur in many networks/societies where constituent nodes/populations directly or indirectly interact with each other. Such phenomena have been observed in various fields such as ecology and evolution [1], dispersive environments resulting in unique spatial patterns among their populations [2], frequency-dependent cancer progression and dynamics [3,4], and collective oscillations in genetic networks [5]. Moreover, during the last few decades, scientists have used these dynamics to describe cognitive processes such as sequential learning and decision making in the brain [6,7]. Such dynamics have been further incorporated in cellular neural networks [8].

To mathematically model the interactions between the populations or nodes of a dynamic network, different models and equation sets have been introduced. One important set of such equations used to express and predict the fate of an ongoing competition in a population of N interacting nodes within a network topology is the set of generalized Lotka–Volterra

(GLV) equations [9–11]. This set of ordinary differential equations has several dynamical solutions corresponding to the results of nodal competitions. By changing the interaction rates between nodes, the Lotka–Volterra equations are capable of producing simple attractors, stable heteroclinic channels (SHCs), limit cycles, and even chaotic solutions. These dynamics have been suggested to model neural population dynamics, as well as single neuronal activities [12]. In the context of laser physics, they have been used to describe the interaction between modes of multimode lasers where modes are coupled to each other through cross-saturation coefficients [13]. However, in multimode lasers, these parameters are inherent to the laser structure and are fixed, preventing us from exploring and switching between different dynamics and, consequently, mapping physical problems onto the system.

In this Letter, we introduce a network consisting of coupled lasers designed so that the rate equations of the semiconductor lasers resemble Lotka–Volterra equations. It should be noted that since semiconductor lasers present a carrier density-dependent refractive index, the phase and amplitude of the optical fields are coupled to each other. Thus, we propose to exploit the physics of a complex amplitude of coupled arrays of laser oscillators to formulate complex Lotka–Volterra (CLV) equations. In such a system, using optoelectronically coupled semiconductor lasers, competitive dynamics can be achieved in an optical platform. On the other hand, lasers with feedbacks are highly nonlinear systems allowing the emergence of more complex dynamical behavior. Here, we investigate different regimes of competition/cooperation among the laser output photon numbers and optical phases. Further, we study the influence of asymmetric coupling strength and frequency detuning between semiconductor lasers and demonstrate winnerless, winner-takes-all (WTA), as well as winner-shares-all (WSA) competitions. We also demonstrate partial synchronization among laser nodes and show bifurcation of heteroclinic channel all the way to a chaotic regime.

The objective of our model is to realize a photonic platform that is governed by Lotka–Volterra equations. To achieve this, we propose a network of N laser nodes interacting via mutually non-symmetric inhibitory connections [see Fig. 1(a)]. These connections are realized through optoelectronic feedback loops [14–17]. We assume that the feedback delay time is negligible,
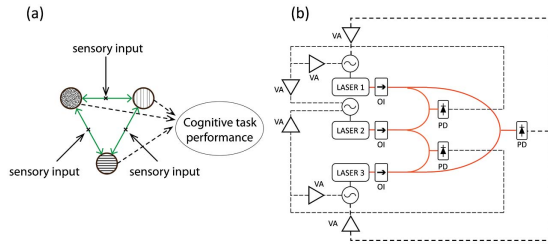
Fig. 1. (a) Network consisting of multiple nodes interacting via inhibitory connections. The sensory input signals affect the control parameters of the system, resulting in the change of the dynamic state of the system. (b) Our proposed scheme: three semiconductor lasers coupled through nonlinear optoelectronic feedbacks. The solid and dashed lines depict the optical and electronic connections; respectively. OI, PD, and VA stand for optical isolator, photodetector, and variable amplifier (attenuator), respectively.

compared to the response time of the system which is a valid assumption for an on-chip realization where the light path and wirings are short [18]. For simplicity, a computational analysis is done for $N = 3$ single mode semiconductor lasers (network's nodes) with independent intrinsic frequencies. In the proposed architecture shown in Fig. 1(b), the heterodyne RF beat notes of each pair of laser outputs, are converted into photocurrent and then added to the bias current of each laser with independent amplification or attenuation (inhibitory connections between network nodes). For the general case of N nodes, the set of coupled rate equations describing the time evolution of the slowly varying, the complex amplitude electric field E_j of emitted radiation from the j-th laser, and its population inversion n_j can be written in the form of a CLV equations as [19]

$$\frac{dE_j}{d\tau} = \frac{\Gamma G_0}{2}(1 + i\alpha)n_j E_j + i(\omega_j - \omega_0)E_j - \mu_j|E_j|^2 E_j, \quad j = 1, \ldots, N, \tag{1}$$

$$\frac{dn_j}{d\tau} = \frac{I_j - I_{th}}{e} - \frac{1}{e}\sum_{\substack{k=1 \\ k \neq j}}^{N} \eta_{jk}(\vec{S})[|E_j|^2 + |E_k|^2$$
$$+ E_j E_k \cos(\Delta\omega_{jk}(\vec{S}) + \varphi_k - \varphi_j)] - \frac{n_j}{\tau_c} - \left(\frac{1}{\Gamma\tau_p} + G_0 n_j\right)|E_j|^2, \tag{2}$$

where Γ is the confinement factor of the laser waveguide, G_0 is the material gain at transparency, α is the linewidth enhancement factor, ω_j is the intrinsic frequency of the laser, ω_0 is the cavity resonance frequency, μ_j is the nonlinear gain self-saturation added to account for the nonlinearity of the gain at high powers [20], I_j and I_{th} are the bias and threshold currents, e is the fundamental electric charge, τ_c and τ_p are the carrier and photon lifetimes, respectively, and $\vec{S}$ is the vector of the time-dependent sensory inputs. η_{jk} and $\Delta\omega_{jk} = \omega_k - \omega_j$ stand for the feedback strength and the frequency detuning between lasers j and k which are sensitive to changes in the sensory input. Furthermore, φ_j is the optical phase of laser j. We have neglected the spontaneous emission coupling into the laser mode for the simplicity of our analysis. The sensory inputs can affect the feedback strength and/or the frequency detuning between the lasers.

By defining $t \equiv \tau/\tau_p$, the dimensionless equations for laser amplitude and phases can be written in the form

$$\frac{dR_j}{dt} = Z_j R_j - \xi_{sj} R_j^3 \qquad j = 1, \ldots, N, \tag{3}$$

$$T\frac{dZ_j}{dt} = P_j - Z_j - (1 + 2Z_j)R_j^2$$
$$- \sum_{\substack{k=1 \\ k \neq j}}^{N} \xi_{jk}(\vec{S})(R_j^2 + R_k^2 + R_j R_k \cos \Psi_{jk}), \tag{4}$$

$$\frac{d\Psi_{jk}}{dt} = \alpha(Z_j - Z_k) + \Omega_{jk}(\vec{S}), \tag{5}$$

where R_j and Z_j are the field amplitude and carrier inversion of laser j, respectively. ξ_{sj}, ξ_{jk}, and Ψ_{jk} are the normalized nonlinear self-saturation, nonlinear optoelectronic feedback coefficients, and phase difference between lasers j and k; respectively. T is the characteristic time of the system defined as the ratio of the carrier and photon lifetimes, P_j is the pump parameter above threshold, and $\Omega_{jk} = (\omega_k - \omega_j)\tau_p$ stands for the detuning between lasers j and k. The parameters used in this Letter are $\xi_{sj} = 5.3 \times 10^{-3}$, $\tau_c = 3$ ns, $\tau_p = 3.3$ ps, $P = 1$, and $\alpha = 4$ for all lasers. The relaxation oscillation frequency of each laser is calculated as $\omega_R = \sqrt{2P/\tau_c\tau_p} \sim 2.25$ GHz.

Next, we investigate the heteroclinic dynamics of such a network of three coupled semiconductor laser oscillators and demonstrate various dynamical regimes. Let us consider the case of three coupled free-running lasers with no external inputs. For $N = 3$ (in the absence of phases), the system of equations (3,4) has seven nontrivial equilibria (fixed points), and the result of competition among lasers relies on the eigenvalues of the linearized system around these points. The nontrivial fixed points of this system include three on R_1, R_2, and R_3 axes (axial fixed points), three on $R_1 R_2$, $R_1 R_3$, and $R_2 R_3$ planes (planar fixed points), and a central fixed point with nonzero values of R_1, R_2, and R_3. Six coupling strength factors between lasers (the extent of amplification/attenuation) and three additional parameters corresponding to their frequency detuning can be used to control the system.

From the point of view of nonlinear dynamics, an important dynamic observed in various applications is winnerless competition (WLC), in which each constituent node is a temporary successive winner in a neverending competition. A mathematical image of such a process is the so-called SHC. The heteroclinic channels appear due to sequential transitioning between saddle equilibria connected through unstable separatrices corresponding to the maximal eigenvalues [11]. The transition between saddle points here can be applied to describe the cyclic switching between different nodal activities. Figure 2(a) shows heteroclinic dynamics of the optical field amplitudes in state space. The result in Fig. 2(a) is obtained for the case in which lasers have zero frequency detuning with coupling coefficients of $\xi_{12} = \xi_{23} = \xi_{31} = 0.45$ and $\xi_{13} = \xi_{21} = \xi_{32} = 0$. It should be noted that the asymmetry of connectivities (i.e., $\xi_{jk} \neq \xi_{kj}$) is a necessity for obtaining SHCs. In this case, all fixed points are saddle with unstable manifolds of dimension two for axial and center fixed points and an unstable manifold of dimension one for planar fixed points. The eigenvalues of the linearized system are -0.0011 (order 2), $-0.0049 \pm 0.0470i$,
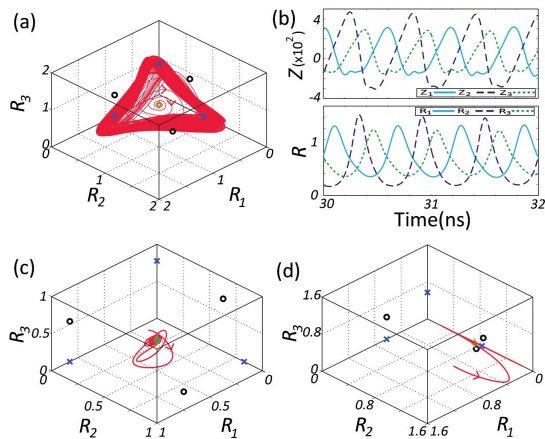
Fig. 2. (a) WLC in the state space of laser optical field amplitudes (R_1, R_2, R_3), where $\xi_{12} = \xi_{23} = \xi_{31} = 0.45$ and $\xi_{13} = \xi_{21} = \xi_{32} = 0$. (b) WLC time series representation of R and Z (transient data is discarded here). (c) WSA when all trajectories converge into one stable fixed point, illustrating the coexistence of three modes ($\xi_{12} = \xi_{23} = \xi_{31} = 0.45$ and $\xi_{13} = 0.2$, $\xi_{21} = \xi_{32} = 0$). (d) WTA in R state space where $\xi_{12} = \xi_{23} = 0.45$, $\xi_{31} = \xi_{21} = 1.6$, and $\xi_{13} == \xi_{32} = 0$. It is assumed that all three lasers have zero detuning. The fixed points of the system are indicated by a blue cross (axial FPs), black circles (plane FPs), and a green diamond (central FP).

1, 0.6923 at the axial, 0.8965, –0.0011, –0.0020 ± 0.0307i, –0.0049 ± 0.0470i at the planar, and –0.0033 ± 0.0471i, –0.0108 ± 0.0363i, 0.0043 ± 0.0363i at the central fixed points.

Interestingly, this heteroclinic channel appears not only among the optical field amplitudes and carrier inversions, but also among the phase differences of the coupled lasers. The existence of robust heteroclinic channel in the phase of oscillators has been mathematically predicted in coupled oscillator networks [21,22], but, to the best of our knowledge, the coexistence of SHC in both intensity and phase dynamics has never been shown before. The time series of the field amplitudes and carrier inversions is shown in Fig. 2(b). This plot shows that the carrier inversions (Z_1, Z_2, Z_3) undergo sequential winnerless switching, and a similar dynamic, delayed by tens of picoseconds, is observed among the optical amplitudes entrained to the carrier inversions. Furthermore, by setting $\xi_{13} = 0.2$, this network can reach the WSA regime where all trajectories converge to a central fixed point, and the resources are shared equally among the competing nodes [Fig. 2(c)]. The behavior of our dynamical system strongly depends on the level of symmetry of the connections among oscillatory elements of the network. Changing asymmetric connections between lasers leads to another interesting dynamic labeled as WTA, wherein the fixed point associated with an amplitude of one of the lasers becomes a global attractor. Such types of dynamics are usually labeled as WTA. This happens when sensory inputs force the inhibitory suppression of all but one modality to become stronger, leading to the allocation of all resources to one modality. Such a regime is represented by a stable fixed point, as shown in Fig. 2(d). It is worth emphasizing that the various dynamics in this Letter are obtained by tuning the control parameters.

All dynamical regimes shown in Fig. 2 are obtained assuming zero frequency detuning between lasers, a challenging condition to achieve experimentally. Thus, it is necessary to

exploit the effect of detuning, considering that it adds extra degrees of freedom for controlling the nonlinear dynamics of our system. Increasing the detuning can lead to period doubling bifurcation at first, and may result in more complex and, even chaotic-like dynamics, if the detuning is increased further. These dynamic behaviors are shown in Fig. 3 in which lasers 1 and 2 have zero detuning ($\Delta\omega_{12} = 0$), and $\Delta\omega_{13}$ is our control parameter. As $\Delta\omega_{13}$ is increased, a stable periodic orbit [Fig. 3(a)] becomes unstable, and an orbit with double the period appears [Fig. 3(b)]. In larger detuning regimes, a period two orbit becomes a period four orbit [Fig. 3(c)] and, finally, a chaotic-like motion appears [Fig. 3(d)]. Such multi-periodic behaviors are essential in describing more complex dynamical processes.

It is worth mentioning that the dynamics of phase differences do not necessarily follow the amplitude dynamics, as shown in Fig. 3. For instance, setting the control parameters as $\xi_{12} = \xi_{23} = \xi_{31} = 0.35$, $\xi_{21} = 0.2$, $\xi_{13} = \xi_{32} = 0$, and $\Delta\omega_{12} = \Delta\omega_{31} = 40$ MHz leads to a limit cycle, modulated with high-frequency fluctuations, as depicted in the amplitude state space in Fig. 4(a). In this case, the state space of the phase differences shows a completely different behavior with an oscillatory trajectory on a plane [Fig. 4(b)]. The behavior of the phases can be better understood through the time series of the phase differences, as shown in Fig. 4(c). The phase differences present plateaus indicating a partial synchronization between the three lasers (phase-locking window) followed by a desynchronization window [23]. In fact, laser 1 is phase locked to laser 2 ($\Psi_{12} = $ const. $\neq 0$) with a jump of 2π after each cycle period, while lasers 1 and 3 are partially synchronized ($\Psi_{31} \approx 0$) [24]. Looking at the amplitudes, the state space diagram one can say that phase locking was achieved over the non-oscillating part of the limit cycle trajectory, while the desynchronization occurs when high-frequency fluctuations appear. Furthermore, by increasing the inhibition connectivity between lasers 1 and 3 to $\xi_{13} = 0.2$, it is possible to increase the phase-locking
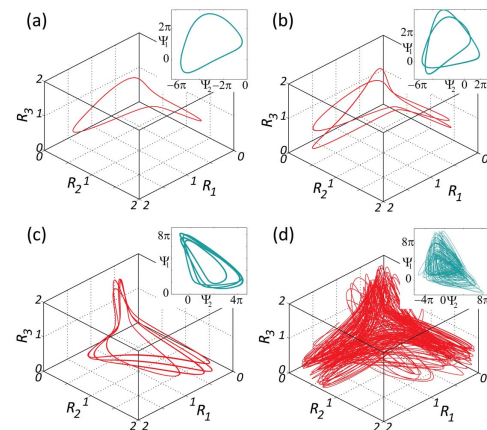
Fig. 3. Bifurcations of field amplitudes and phase differences (shown in the inset) achieved by increasing the control parameter $\Delta\omega_{31}$. Transient data have been discarded in these figures. The parameters used are $\xi_{12} = \xi_{23} = \xi_{31} = 0.75$ and $\xi_{13} = \xi_{21} = \xi_{32} = 0$. Lasers 1 and 2 have zero detuning, and the third laser has a detuning of $\Delta\omega_{13}$ with respect to them. $\Delta\omega_{13}$ is increased, and the state space of an (a) initially periodic signal ($\Delta\omega_{13} = 0$ MHz) undergoes successive bifurcations such as (b) period-doubling ($\Delta\omega_{13} = 20$ MHz) and (c) period four orbits ($\Delta\omega_{13} = 99$ MHz), and eventually becomes (d) chaotic-like ($\Delta\omega_{13} = 108$ MHz).
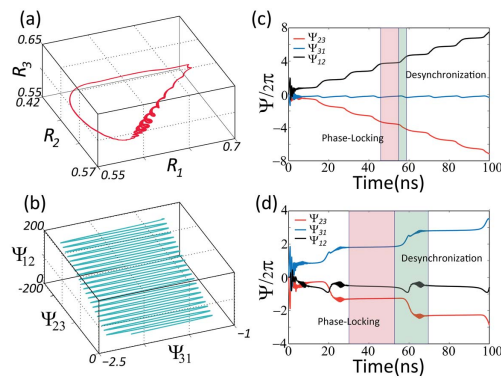
Fig. 4. Partial phase synchronization regime. (a) Amplitude state space where $\xi_{12} = \xi_{23} = \xi_{31} = 0.35$, $\xi_{13} = \xi_{32} = 0$, $\xi_{21} = 0.2$ and $\Delta\omega_{12} = \Delta\omega_{31} = 40$ MHz; (b) phase difference state space; (c) time series representation of normalized phase differences; and (d) time series representation of normalized phase differences where $\xi_{12} = \xi_{23} = \xi_{31} = 0.35$, $\xi_{21} = \xi_{13} = 0.2$, $\xi_{32} = 0$, and $\Delta\omega_{12} = \Delta\omega_{31} = 40$ MHz.

window to be much longer than the bubbling event, as shown in Fig. 4(d). The synchronization mechanism is a characteristic feature of large-scale networks, where it can be utilized to trigger synchronized activities among different elements, as well as different layers of the network.

In conclusion, in this Letter, we present GLV dynamical solutions as applied to a photonics network consisting of optoelectronically cross-coupled semiconductor lasers. In such a network, the interaction of intensity and carrier inversion rates, as well as the phases of laser nodes, results in various solutions. We demonstrate the influence of asymmetric coupling strengths and frequency detuning between lasers. It has been demonstrated that asymmetric inhibitory connections between different nodes are essential to achieving sequential amplitude oscillations of laser nodes (WLC regime) and lead to both a sensitive and stable network. It is worth noting that the strength of feedback to one of the constituent lasers must be much larger than the feedbacks to the rest in order for one of them to win the competition and, consequently, for the system to reach a stable state regime. Furthermore, in order to avoid the chaotic regime, small coupling coefficients (relative to the pumping power of each laser) have to be used. A system with large coupling coefficients is inherently highly sensitive to frequency detuning. Numerical simulations additionally indicate that a variety of dynamical behaviors, including higher-order heteroclinic cycles can be observed in such a network. Finally, we have also demonstrated partial synchronization between laser nodes which facilitates any future large scale integration [25]. Further studies are required to address additional properties of our system such as a system's stability with respect to phase and intensity noise and system's response time for sensory inputs.

This Letter was primarily motivated with an aim to pursue the optical implementation of a processor that is inspired by brain dynamics using nonlinearly coupled semiconductor laser oscillators with a programmable strength of interaction. According to studies that model brain dynamics, the dynamical principles of SHCs can be the basic mechanism for sequential information processing and robust representation of transient cognitive modal dynamics [26]. A simple mathematical model to implement SHCs is indeed the set of GLV equations that are

modeled here. In an optical platform, lasers are suitable nonlinear components with extremely dynamical behavior when coupled properly. However, processing real-world big data will require processors with a substantial number of nonlinearly coupled interacting laser nodes. We envision a scalable and, hence, practical implementation of our system based on a hybrid integration of III/V and silicon photonics chips interconnected via an electronics controller. It should be noted that what we have introduced here is a building block of a complex network with the capabilities of decision making and associative memory [27]. In general, as shown in [7], these small blocks could be arranged in different hierarchical levels to perform more complex cognitive tasks.

REFERENCES

1. J. Hofbauer and K. Sigmund, *Evolutionary Games and Population Dynamics* (Cambridge University, 1998).
2. G. Károlyi, Z. Neufeld, and I. Scheuring, J. Theor. Biol. **236**, 12 (2005).
3. P. M. Altrock, L. L. Liu, and F. Michor, Nat. Rev. Cancer **15**, 730 (2015).
4. J. M. Pacheco, F. C. Santos, and D. Dingli, Interface Focus **4**, 20140019 (2014).
5. F. Mori and A. S. Mikhailov, Phys. Rev. E **062206**, 1 (2016).
6. M. I. Rabinovich, A. Volkovskii, P. Lecanda, R. Huerta, H. D. Abarbanel, and G. Laurent, Phys. Rev. Lett. **87**, 068102 (2001).
7. M. I. Rabinovich, P. Varona, I. Tristan, and V. S. Afraimovich, Front. Comput. Neurosci. **8**, 22 (2014).
8. M. I. Rabinovich, R. Huerta, P. Varona, and V. S. Afraimovich, PLoS Comput. Biol. **4**, e1000072 (2008).
9. P. Arena, L. Fortuna, D. Lombardo, L. Patan, and M. G. Velarde, Int. J. Circ. Theor. Appl. **37**, 505 (2009).
10. M. I. Rabinovich, M. K. Muezzinoglu, I. Strigo, and A. Bystritsky, PLoS One **5**, e12547 (2010).
11. V. Afraimovich, I. Tristan, R. Huerta, and M. I. Rabinovich, Chaos **18**, 043103 (2008).
12. T. Fukai, Neural Comput. **9**, 77 (1997).
13. W. E. Lamb, Phys. Rev. **134**, A1429 (1964).
14. F. Lin and J. Liu, IEEE J. Quantum Electron. **39**, 562 (2003).
15. P. Saboureau, J. Foing, and P. Schanne, IEEE J. Quantum Electron. **33**, 1582 (1997).
16. H. D. I. Abarbanel, M. B. Kennel, L. Illing, S. Tang, H. F. Chen, and J. M. Liu, IEEE J. Quantum Electron. **37**, 1301 (2001).
17. M. C. Soriano, J. García-Ojalvo, C. R. Mirasso, and I. Fischer, Rev. Mod. Phys. **85**, 421 (2013).
18. G. Chen, H. Chen, M. Haurylau, N. A. Nelson, D. H. Albonesi, P. M. Fauchet, and E. G. Friedman, Integr. VLSI J. **40**, 434 (2007).
19. T. Erneux and P. Glorieux, *Laser Dynamics* (Cambridge University, 2010).
20. G. P. Agrawal, IEEE J. Quantum Electron. **23**, 860 (1987).
21. D. Hansel, G. Mato, and C. Meunier, Phys. Rev. E **48**, 3470 (1993).
22. P. Ashwin and J. Borresen, *Nonlinear Dynamics and Chaos: Advances and Perspectives, Understanding Complex Systems* (Springer, 2010).
23. J. Tiana-Alsina, K. Hicke, X. Porte, M. C. Soriano, M. C. Torrent, J. Garcia-Ojalvo, and I. Fischer, Phys. Rev. E **85**, 026209 (2012).
24. M. G. Rosenblum, A. S. Pikovsky, and J. Kurths, Phys. Rev. Lett. **76**, 1804 (1996).
25. L. F. Abbott, J. Phys. A **23**, 3835 (1990).
26. S. J. Kiebel, K. von Kriegstein, J. Daunizeau, and K. J. Friston, PLoS Comput. Biol. **5**, e1000464 (2009).
27. P. Seliger, L. S. Tsimring, and M. I. Rabinovich, Phys. Rev. E **67**, 011905 (2003).